

Polymer Chemistry

Accepted Manuscript



This is an *Accepted Manuscript*, which has been through the Royal Society of Chemistry peer review process and has been accepted for publication.

Accepted Manuscripts are published online shortly after acceptance, before technical editing, formatting and proof reading. Using this free service, authors can make their results available to the community, in citable form, before we publish the edited article. We will replace this *Accepted Manuscript* with the edited and formatted *Advance Article* as soon as it is available.

You can find more information about *Accepted Manuscripts* in the [Information for Authors](#).

Please note that technical editing may introduce minor changes to the text and/or graphics, which may alter content. The journal's standard [Terms & Conditions](#) and the [Ethical guidelines](#) still apply. In no event shall the Royal Society of Chemistry be held responsible for any errors or omissions in this *Accepted Manuscript* or any consequences arising from the use of any information it contains.



Polymer Chemistry

COMMUNICATION

Sub-20 nm Nontoxic Aggregation-Induced Emission Micellar Fluorescent Light-up Probe for Highly Specific and Sensitive Mitochondrial Imaging of Hydrogen Sulfide

Received 00th January 20xx,
Accepted 00th January 20xx

DOI: 10.1039/x0xx00000x

Lei Liu, Bo Wu, Ping Yu, Ren-Xi Zhuo, and Shi-Wen Huang*

www.rsc.org/polymers

A salicyladazine-based amphiphilic polymer (AIE-1) with AIE characteristics was synthesized and self-assembled to form sub-20 nm micelles (AIE-M). The green fluorescence of AIE-M was completely quenched by Cu²⁺ and then recovered with Na₂S, which was utilized for the specific and sensitive detection of S²⁻ in solution and mitochondrial imaging of H₂S in HeLa cells.

Hydrogen sulfide (H₂S), with unpleasant smell of rotten eggs, has been known for long time as a toxic molecule. Until a decade ago, H₂S has been recognized to play an important role in human body and other biological system and regarded as the third gaseous signal molecule along with nitric oxide (NO) and carbon monoxide (CO).¹⁻³ Many analytical methods, including colorimetric, electrochemical, and gas chromatography assays, have been developed to detect H₂S.⁴⁻⁶ Among the current methods, up to now, fluorescent probes-based methods are the most suitable for highly sensitive, highly specific and fast detection of H₂S, especially for the real-time imaging of H₂S in living cells. The unique reactivity properties of H₂S have been utilized to react with nonfluorescence or weak fluorescence small molecules to produce turn-on fluorescence inside the cells, mainly including H₂S-mediated reduction of aryl azide,⁷⁻¹⁰ arylsulfonyl azide,¹¹⁻¹² nitro group,¹³ or azo group,¹⁴ precipitation of Cu²⁺ with H₂S,¹⁵⁻¹⁸ disulfide exchange,¹⁹ and nucleophilic addition,²⁰⁻²² etc. In some cases, significant interference from other biological thiol, such as glutathione (GSH), was found. Organelle-specific imaging of H₂S with fluorescent probes, such as lysosomal-targeting imaging²³⁻²⁴ and mitochondrial-targeting imaging,²⁵⁻²⁸ is of interest and especially appreciated for the investigation of H₂S biology in these organelles.

The traditional fluorescent probes often show aggregation-caused quenching (ACQ) in high-concentration solution *via* the formation of aggregates, which results in weak fluorescence or nonfluorescence of probes in concentrated solution. Different from ACQ of traditional fluorescent probes, aggregation-induced emission (AIE),

which was first discovered by Tang group one decade ago, represents a completely opposite fluorescent phenomena, namely, a fluorogenic molecule shows no emission in molecularly dissolved state but strong emission in aggregation state. Then, much efforts have been made for the design of new AIE molecules, explanation of AIE mechanism and exploring of AIE application.²⁹⁻³⁰ AIE-based bioprobes have been attracted more and more attention in fluorescent sensing and fluorescent imaging, including DNA, proteins, enzymes and small biomolecules.³¹⁻³² Similar to traditional fluorescent probes, most reported AIE-based bioprobes are hydrophobic and thus formed nanosized AIE-dots are not stable enough in biological fluids and limited in bioimaging application. Wei group have made efforts to construct water-dispersible and stable AIE-based nanoprobe with relatively large sizes by PEGylation or conjugating AIE units to amphiphilic polymer for cell imaging.³³⁻³⁴ Liu group have prepared ultrabright AIE-based organic dots encapsulated in micelles for targeted cell imaging.³⁵ However, it is emergent to develop small sized, water-dispersible and highly stable AIE-based bioprobes in biological environment for the detection or imaging of biomolecules, especially for imaging biomolecules in organelles.

A few years ago, salicyladazine was found to show AIE characteristics. Salicyladazine is composed of two salicylaldimine moieties containing intramolecular hydrogen bonds to ensure that N-N bonds are allowed to rotate when dissolved in good solvent, such as ethanol, which results in no fluorescence or weak fluorescence. When aggregation of salicyladazine occurs such as in ethanol/H₂O mixed solvent, the rotation of N-N bonds has been limited, and results in strong fluorescence. Easy and selective modification of hydroxyl groups in salicyladazine with 2,4-dinitrobenzene sulfonyl (DNBS) group, acyl group, allyl group, etc, made it possible for selective detection and imaging of thiol, esterase and Pd inside cells.³⁶⁻⁴⁰ We here report a simple strategy for the design of amphiphilic salicyladazine-based AIE molecule (AIE-1) by separately conjugating hydrophobic segment (long chain alkyl group) and hydrophilic segment (polyethylene glycol, PEG) with the two ends of AIE unit. Fortunately, amphiphilic salicyladazine (AIE-1) not only maintains the AIE characteristics but also forms sub-20 nm micelles (AIE-M) with high storage stability

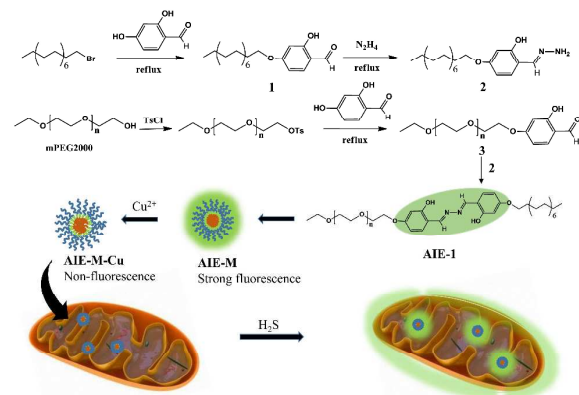
Key Laboratory of Biomedical Polymers of Ministry of Education, and Department of Chemistry, Wuhan University, Wuhan 430072, China.

E-Mail: shwuhuang@whu.edu.cn

Electronic Supplementary Information (ESI) available. See

DOI: 10.1039/x0xx00000x

after dropwise adding the DMSO solution of amphiphilic salicyladazine into water or even only after ultrasonic treatment of amphiphilic salicyladazine solid dispersed in water. **AIE-M** was found to be uptaken by HeLa cells and gradually accumulated in mitochondrion of HeLa cells. The fluorescence of **AIE-M** is quenched by Cu^{2+} via the coordination of **AIE-M** and Cu^{2+} to form **AIE-M-Cu** nanomicelles. Further removal of Cu^{2+} from **AIE-M-Cu** with S^{2-} resulted in the recovery of fluorescence via the fast and S^{2-} -specific conversion of **AIE-M-Cu** to **AIE-M**. Based on these observations, we developed a micellar aggregation-induced emission probe for the imaging of H_2S in mitochondrion of living cells via incubation of cells sequentially with **AIE-M-Cu** and Na_2S .



As shown in scheme 1, the amphiphilic polymer **AIE-1** was synthesized starting from 2,4-dihydroxybenzaldehyde. The separate introduction of long-chain alkyl group (C16) and methyl polyethylene glycol (mPEG) into the 4-hydroxy group of 2,4-dihydroxybenzaldehyde realized the hydrophobization and hydrophilization of the intermediate molecule. **AIE-1** was obtained by the sequential reaction of hydrazine with 2-hydroxy,4-palmitoyloxy benzene aldehyde and 2-hydroxy,4-mPEG-oxy benzene aldehyde. The chemical structures of intermediates and targeting molecule **AIE-1** were confirmed with FTIR and NMR spectroscopy (Figure S1-S8). HPLC analysis indicated that **AIE-1** is stable after incubation separately in pH 7.4, 6.5 or 5.0 buffer for 24 h (Figure S9).

Due to the amphiphilic property of **AIE-1**, it is expected to self-assemble to form nano micelles in aqueous solution. The critical micelle concentration (CMC) of **AIE-1**, measured by a standard method, is $26 \mu\text{g mL}^{-1}$ (Figure S10). Interestingly, small micelles (**AIE-M**) with average size of 18 nm (sub-20 nm) were obtained by dropwise addition of **AIE-1** solution in DMSO into water or even simple ultrasonic treatment of **AIE-1** solid in water. Thus obtained **AIE-M** is highly stable in water and PBS buffer (pH 7.4) even after storage for two weeks (Figure S11). The high stability of **AIE-M** is very important and ideal for the application in biological system.

The photophysical properties of **AIE-1** shown in figure S13 indicated that the maximum absorption wavelength of **AIE-1** in

DMSO is 375 nm in the UV/Vis absorption spectrum, while almost no fluorescence was detected after the excitation of **AIE-1** in DMSO with 408 nm laser. However, when water was added into the solution of **AIE-1** in DMSO, strong fluorescence was detected even in the mixed solvent of DMSO/ H_2O (8:2 v/v), which is a typical characteristic of aggregation-induced emission (Figure 1A). According to the classic method, fluorescence quantum yield ($\text{Y}_f = 0.14$) was calculated using the standard reference sample that has a fixed and known FL QY value.

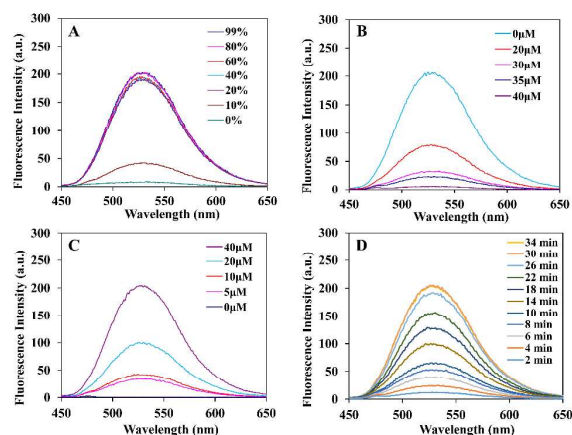


Figure 1 (A) Fluorescence spectra of 40 μM **AIE-1** in mixture solution containing DMSO and water. (B) Fluorescence spectra of 40 μM **AIE-M** treated with Cu^{2+} at 0–40 μM in 0.01 M PBS buffer (pH 7.4) for 30 min. (C) Fluorescence spectra of 40 μM **AIE-M-Cu** treated with Na_2S at 0–40 μM in PBS for 30 min. (D) Time-dependent fluorescence spectra of 40 μM **AIE-M-Cu** treated with 50 μM Na_2S in PBS. $\lambda_{\text{exc}} = 408 \text{ nm}$.

It is well known that the chelating groups in a fluorescent probe form stable complexes with Cu^{2+} , which often show quenching effect on the fluorescence of the probe. There are two salen groups in each molecule of **AIE-1**. We found that the fluorescence of **AIE-M-Cu** aqueous solution, prepared by adding Cu^{2+} to **AIE-M** aqueous solution, gradually decreased and completely quenched after adding equivalent Cu^{2+} , which is believed due to the formation of stable Cu^{2+} complexes (**AIE-M-Cu**) with salen groups in **AIE-M** and the paramagnetic Cu^{2+} center partly or fully quenched the fluorescence of **AIE-M** (Figure 1B).

Precipitation of Cu^{2+} from the Cu^{2+} -fluorescent probe complexes with S^{2-} are often utilized for S^{2-} sensing and imaging because of the high affinity of S^{2-} for Cu^{2+} , which will result in the fluorescence recovery of a probe. Na_2S as the aqueous resource of S^{2-} , at concentration ranging from 5–40 μM , was added to **AIE-M-Cu** aqueous solution (containing 40 μM of salicyladazine unit) with almost no fluorescence, a large and fast increment of fluorescence intensity by 50–400 folds were observed within 30 min, which relied on the addition amount of Na_2S (Figure 1C). The complete recovery of fluorescence from **AIE-M-Cu** to **AIE-M** finished within 30 min after treatment with Na_2S (Figure 1D). In contrast, other anions, such as

Cl^- , CO_3^{2-} , NO_3^- , PO_4^{3-} , H_2PO_4^- , $\text{S}_2\text{O}_3^{2-}$, SO_3^{2-} , and biothiols, such as cysteine, GSH, showed no effect on the fluorescence increment of **AIE-M-Cu** (Figure S14). This means **AIE-M-Cu** offers the high selectivity for H_2S sensing *via* CuS precipitation.

The high selectivity, sensitivity of **AIE-M-Cu** for H_2S sensing and its high storage stability encourages us to explore its application in imaging H_2S in living cells. Prior to cell imaging, we first evaluated the cytotoxicity of **AIE-M** and **AIE-M-Cu** against HeLa cells using MTT assay. The results indicated that **AIE-M** and **AIE-M-Cu** are almost nontoxic to HeLa cells even at a relatively high concentration of $500 \mu\text{g mL}^{-1}$ (Figure S15). The membrane permeability of a fluorescent probe is also an important consideration for cell imaging. Because **AIE-M-Cu** is nonfluorescent, **AIE-M**, instead of **AIE-M-Cu**, was used for cellular uptake evaluation. After 4 h or 8 h incubation of HeLa cells with **AIE-M** (containing $40 \mu\text{M}$ or $80 \mu\text{M}$ of salicyladazine unit), strong green fluorescence was observed inside HeLa cells, especially for 8 h incubation, which is sufficient for cell imaging (Figure 2A-2D). We further studied the intracellular localization of **AIE-M** in HeLa cells. After 8 h incubation of HeLa cells with **AIE-M**, the cells were co-stained with Mitotracker (a mitochondrial staining) or Lysotracker (a lysosomal staining). CLSM analysis shows green fluorescence from **AIE-M** is well overlapped with red fluorescence from Mitotracker (Figure 2F), while less overlap between **AIE-M** and Lysotracker fluorescence signal was observed (Figure 2E). Calculated pearson's correlation coefficients for **AIE-M** in mitochondria and lysosomes were 0.751 and 0.187 respectively. The results demonstrated the excellent localization ability of **AIE-M** in mitochondrion of HeLa cells, which is possibly ascribed to the ultrasmall size (sub-20 nm) of **AIE-M**. Although we did not have sufficient evidences to explain the mitochondrial accumulation of **AIE-M** in HeLa cells, similar phenomenon, the increased mitochondrial accumulation of sub-12 nm polymeric micelles in cells, has been observed previously.⁴¹

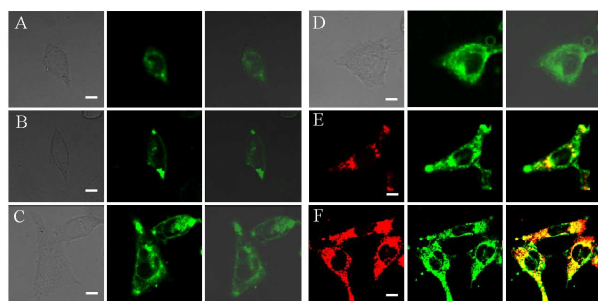


Figure 2 (1) CLSM images of HeLa cells after incubation with **AIE-M**. In brief, HeLa cells were incubated with $40 \mu\text{M}$ (A, C) or $80 \mu\text{M}$ (B, D) **AIE-M** for 4 h (A, B) or 8 h (C, D). (2) CLSM images of HeLa cells after incubation with **AIE-M** ($40 \mu\text{M}$). HeLa cells were incubated with **AIE-M** ($40 \mu\text{M}$) for 8 h, and then co-stained with 100 nM lysotracker (E) or 200 nM mitotracker (F) after washed with PBS. $\lambda_{\text{ex}} = 408 \text{ nm}$. Scale bar = $40 \mu\text{m}$.

We next tested the application of **AIE-M-Cu** in visualizing H_2S in living cells. After 8 h incubation of **AIE-M-Cu** containing $40 \mu\text{M}$ of salicyladazine unit in complete cell culture medium, the medium

was replaced with fresh serum-free medium containing $50 \mu\text{M}$ of Na_2S . The cells were immediately observed with CLSM upon the excitation at 408 nm or after further incubation for 5, 10 20, and 30 min, and then observed (Figure S16). There is no fluorescence observed for cells alone or in the case of immediate observation once Na_2S was added into the cell culture medium. After incubation of HeLa cells in Na_2S -containing medium, the fluorescence gradually appeared and increased with the increase of incubation time, and strong green fluorescence was seen after 30-min incubation. The imaging of H_2S in HeLa cells with **AIE-M-Cu** is fast, and the intensity of green fluorescence in HeLa cells after the uptake of **AIE-M-Cu** and subsequent treatment with Na_2S for 30 min was comparable to that of the same amount of **AIE-M** treated HeLa cells. This means the almost complete recovery of fluorescence inside cells of **AIE-M** converting from **AIE-M-Cu** treated with Na_2S within 30 min. The cell imaging results are consistent with the results in Figure 1D.

To explore the detection limitation of exogenous Na_2S concentration in cell culture medium, HeLa cells were cultured with **AIE-M-Cu** at a concentration of $40 \mu\text{M}$ salicyladazine unit, and various concentration of Na_2S ($0, 5, 10, 20, 40,$ and $80 \mu\text{M}$) was separately added into the cell culture wells and cultured for further 30 min. From the CLSM observation, it was found that relatively weak green fluorescence was observed in HeLa cells even the concentration of Na_2S in culture medium was as low as $10 \mu\text{M}$.

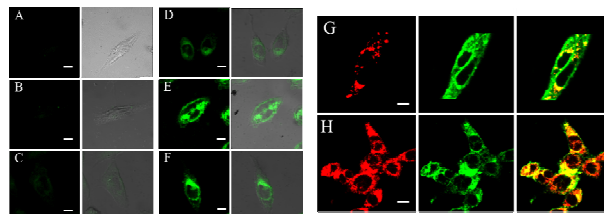


Figure 3 (1) CLSM images of HeLa cells after incubation with different concentration of Na_2S . HeLa cells were incubated with **AIE-M-Cu** ($40 \mu\text{M}$) for 8 h, after washed with PBS, $0 \mu\text{M}$ (A), $5 \mu\text{M}$ (B), $10 \mu\text{M}$ (C), $20 \mu\text{M}$ (D), $40 \mu\text{M}$ (E), $80 \mu\text{M}$ (F) of Na_2S was added to incubate with cells for 30 min. (2) CLSM images of HeLa cells after incubation with Na_2S ($100 \mu\text{M}$). HeLa cells were incubated with **AIE-M-Cu** ($40 \mu\text{M}$) for 8 h, $100 \mu\text{M}$ of Na_2S was then added. After 30 min incubation, the cells were stained with 100 nM lysotracker (G) or 200 nM mitotracker (H). $\lambda_{\text{ex}} = 408 \text{ nm}$. Scale bar = $40 \mu\text{m}$.

The intracellular fluorescence localization of **AIE-M-Cu** treated with Na_2S was also investigated by co-staining with Mitotracker or Lysotracker (Figure 3). Similar to **AIE-M** alone, the fluorescence in HeLa cells sequentially treated with **AIE-M-Cu** and Na_2S also localized in mitochondria. Excellent overlap between green fluorescence from **AIE-M** converting from **AIE-M-Cu** and red fluorescence from Mitotracker (Figure 3H), and poor overlap between green fluorescence from **AIE-M** and red fluorescence from Lysotracker (Figure 3G) was separately observed. Calculated

pearson's correlation coefficients for AIE-M-Cu in mitochondria and lysosomes were 0.763 and 0.256 respectively. This suggested the mitochondrial H₂S in HeLa cells be imaged after incubation of HeLa cells sequentially with AIE-M-Cu and Na₂S.

Conclusions

In summary, we have designed and synthesized an amphiphilic polymer (AIE-1) with aggregation-induced emission characteristics. The strong green fluorescence of uniformly sized and highly storage stable nano micelles (AIE-M), prepared from AIE-1 by simple ultrasonic treatment of solid AIE-1 in water, buffer, or cell culture medium, can be quickly quenched by Cu²⁺ based on the formation of complexes between Cu²⁺ and salen groups in salicylazadiazine unit of AIE-1. The selective and sensitive fluorescence recovery of AIE-M-Cu with Na₂S can be applied in the detection of S²⁻ in solution. Furthermore, fast and sensitive fluorescence imaging of mitochondrial H₂S can be realized in HeLa cells by prior cellular uptake of AIE-M-Cu and succedent incubation with Na₂S. We anticipate that this new AIE-based micelles, integrating small sizes, high stability, nontoxicity, and mitochondrial accumulation ability, will be valuable for exploring a wide range of biological function of H₂S.

Acknowledgements

This work was financially supported by National Natural Science Foundation of China (51473127, 51273150).

Notes and references

- 1 C. Szabo, *C. Nat. Rev. Drug Discov.*, 2007, **6**, 917-935.
- 2 G. D. Yang, L. Y. Wu, B. Jiang, W. Yang, J. S. Qi, K. Cao, Q. H. Meng, A. K. Mustafa, W. T. Mu, S. M. Zhang, S. H. Snyder, R. Wang, *Science*, 2008, **322**, 587-590.
- 3 H. Kimura, *Amino Acids*, 2011, **41**, 113-121.
- 4 V. S. Lin, W. Chen, M. Xian, C. J. Chang, *Chem. Soc. Rev.*, 2015, DOI: 10.1039/C4CS00298A.
- 5 V. S. Lin, C. J. Chang, *Current Opin. Chem. Biol.*, 2012, **16**, 595-601.
- 6 F. B. Yu, X. Y. Han, L. X. Chen, *Chem. Commun.*, 2014, **50**, 12234-12249.
- 7 A. R. Lippert, E. J. New, C. J. Chang, *J. Am. Chem. Soc.*, 2011, **133**, 10078-10080.
- 8 S. Chen, Z. J. Chen, W. Ren, H. W. Ai, *J. Am. Chem. Soc.*, 2012, **134**, 9589-9592.
- 9 V. S. Lin, A. R. Lippert, C. J. Chang, *Proc. Natl. Acad. Sci. USA*, 2013, **110**, 7131-7135.
- 10 Z. J. Chen, W. Ren, H. W. Ai, *Biochem.*, 2014, **53**, 5966-5974.
- 11 W. M. Xuan, C. Q. Sheng, Y. T. Cao, W. H. He, W. Wang, *Angew. Chem. Int. Ed.*, 2012, **51**, 2282-2284.
- 12 H. J. Peng, Y. F. Cheng, C. F. Dai, A. L. King, B. L. Predmore, D. J. Lefer, B. H. Wang, *Angew. Chem. Int. Ed.*, 2011, **50**, 9672-9675.
- 13 A. Montoya, M. D. Pluth, *Chem. Commun.*, 2012, **48**, 4767-4769.
- 14 X. Li, J. Cheng, Y. L. Gong, B. Yang, Y. Z. Hu, *Biosens. Bioelectron.*, 2015, **65**, 302-306.
- 15 M. G. Choi, S. Cha, H. Lee, H. L. Jeon, S. K. Chang, *Chem. Commun.*, 2009, **47**, 7390-7392.
- 16 K. Sasakura, K. Hanaoka, N. Shibuya, Y. Mikami, Y. Kimura, T. Komatsu, T. Ueno, T. Terai, H. Kimura, T. Nagano, *J. Am. Chem. Soc.*, 2011, **133**, 18003-18005.
- 17 X. Li, C. Y. Yang, K. Wu, Y. Z. Hu, S. F. Han, S. H. Liang, *Theranostics*, 2014, **4**, 1233-1238.
- 18 X. Li, Y. L. Gong, K. Wu, S. H. Liang, J. Cao, B. Yang, Y. Z. Hu, S. F. Han, *RSC Adv.*, 2014, **4**, 36106-36109.
- 19 C. R. Liu, J. Pan, S. Li, Y. Zhao, L. Y. Wu, C. E. Berkman, A. R. Whorton, M. Xian, *Angew. Chem. Int. Ed.*, 2011, **50**, 10327-10329.
- 20 C. R. Liu, B. Peng, S. Li, C. M. Park, A. R. Whorton, M. Xian, *Org. Lett.*, 2012, **14**, 2184-2187.
- 21 S. Singha, D. Kim, H. Moon, T. Wang, K. H. Kim, Y. H. Shin, J. Jung, E. Seo, S. J. Lee, K. H. Ahn, *Anal. Chem.*, 2015, **87**, 1188-1195.
- 22 Y. Qian, J. Karpus, O. Kabil, S. Y. Zhang, H. L. Zhu, R. Banerjee, J. Zhao, C. He, *Nature Commun.*, 2011, **2**, 495.
- 23 T. Y. Liu, Z. C. Xu, D. R. Spring, J. N. Cui, *Org. Lett.*, 2013, **15**, 2310-2313.
- 24 Q. L. Qiao, M. Zhao, H. J. Lang, D. Q. Mao, J. N. Cui, Z. C. Xu, *RSC Adv.*, 2014, **4**, 25790-25794.
- 25 Y. C. Chen, C. C. Zhu, Z. H. Yang, J. J. Chen, Y. F. He, Y. Jiao, W. J. He, L. Qiu, J. J. Cen, Z. J. Guo, *Angew. Chem. Int. Ed.*, 2013, **52**, 1688-1691.
- 26 X. Chen, S. Q. Wu, J. H. Han, S. F. Han, *Bioorg. Med. Chem. Lett.*, 2013, **23**, 5295-5299.
- 27 X. L. Liu, X. J. Du, C. G. Dai, Q. H. Song, *J. Org. Chem.*, 2014, **79**, 9481-9489.
- 28 M. Gao, F. B. Yu, H. Chen, L. X. Chen, *Anal. Chem.*, 2015, **87**, 3631-3638.
- 29 R. R. Hu, N. L. C. Leung, B. Z. Tang, *Chem. Soc. Rev.*, 2014, **43**, 4494-4562.
- 30 J. Mei, Y. N. Hong, J. W. Y. Lam, A. J. Qin, Y. H. Tang, B. Z. Tang, *Adv. Mater.*, 2014, **26**, 5429-5479.
- 31 D. Ding, K. Li, B. Liu, B. Z. Tang, *Acc. Chem. Res.*, 2013, **46**, 2441-2453.
- 32 J. Liang, B. Z. Tang, B. Liu, *Chem. Soc. Rev.*, 2015, **44**, 2798-2811.
- 33 X. Y. Zhang, X. Q. Zhang, B. Yang, J. F. Hui, M. Y. Liu, W. Y. Liu, Y. W. Chen, Y. Wei, *Polym. Chem.*, 2014, **5**, 689-693.
- 34 H. Y. Liang, X. Q. Zhang, X. Y. Zhang, B. Yang, Y. Yang, Y. Wei, *Polym. Chem.*, 2014, **5**, 3758-3762.
- 35 G. L. Geng, K. Li, D. Ding, X. H. Zhang, W. Qin, J. Z. Liu, B. Z. Tang, B. Liu, *Small*, 2012, **8**, 3655-3663.
- 36 W. X. Tang, Y. Xiang, A. J. Tong, *J. Org. Chem.*, 2009, **74**, 2163-2166.
- 37 L. Peng, Z. J. Zhou, R. R. Wei, K. Li, P. S. Song, A. J. Tong, *Dyes Pigm.*, 2014, **108**, 24-31.
- 38 M. Gao, C. K. Sim, C. W. T. Leung, Q. L. Hu, G. X. Feng, F. Xu, B. Z. Tang, B. Liu, *Chem. Commun.*, 2014, **50**, 8312-8315.
- 39 Q. L. Hu, M. Gao, G. X. Feng, B. Liu, *Angew. Chem. Int. Ed.*, 2014, **53**, 14225-14229.
- 40 R. Y. Zhang, M. Gao, S. Q. Bai, B. Liu, *J. Mater. Chem.*, 2015, **3**, 1590-1596.
- 41 K. Chong, T. Ku, P. E. Saw, S. Jon, J. H. Park, C. Choi, *Chem. Commun.*, 2013, **49**, 11476-11478.